Photophysics of Voltage Increase by Photoinduced Dipole Layers in Sensitized Solar Cells

ARTICLE *in* JOURNAL OF PHYSICAL CHEMISTRY LETTERS · AUGUST 2014

Impact Factor: 7.46 · DOI: 10.1021/jz501336r

6 AUTHORS, INCLUDING:

Miri Kazes
Weizmann Institute of Science
18 PUBLICATIONS **1,445** CITATIONS
SEE PROFILE

Ohr Lahad
Weizmann Institute of Science
3 PUBLICATIONS **6** CITATIONS
SEE PROFILE

Arie Zaban
Bar Ilan University
170 PUBLICATIONS **10,728** CITATIONS
SEE PROFILE

THE JOURNAL OF PHYSICAL CHEMISTRY Letters

Letter

pubs.acs.org/JPCL

Photophysics of Voltage Increase by Photoinduced Dipole Layers in Sensitized Solar Cells

Miri Kazes,[§,†] Sophia Buhbut,[§,‡] Stella Itzhakov,[†] Ohr Lahad,[†] Arie Zaban,[‡] and Dan Oron*[,†]

[†]Department of Physics of Complex Systems, Weizmann Institute of Science, Rehovot 76100, Israel

[‡]Department of Chemistry, Bar Ilan University, Ramat-Gan 52900, Israel

Supporting Information

ABSTRACT: Significant overpotentials between the sensitizer and both the electron and hole conductors hamper the performance of sensitized solar cells, leading to a reduced photovoltage. We show that by using properly designed type-II quantum dots (QDs) between the sensitizer and the hole conductor in thin absorber cells, it is possible to increase the open circuit voltage (V_{oc}) by more than 100 mV. This increase is due to the formation of a photoinduced dipole (PID) layer. Photogenerated holes in the type-II QDs are retained in the core for a relatively long time, allowing for the accumulation of a positively charged layer. Negative charges are, in turn, injected and accumulated in the TiO_2 anode, creating a dipole moment, which negatively shifts the TiO_2 conduction band relative to the electrolyte. We study this phenomenon using a unique TiO_2/CdSe/(ZnSe:Te/CdS)/polysulfide system, where the formation of a PID depends on the color of the illumination. The PID concept thus introduces a new design strategy, where the operating parameters of the solar cell can be manipulated separately.

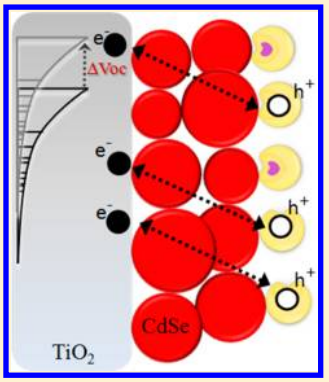

SECTION: Energy Conversion and Storage; Energy and Charge Transport

One of the main problems limiting the performance of sensitized solar cells is the band alignment between the selective contacts and the sensitizer. When the overpotential between the sensitizer and the selective contact is excessive, the maximum possible output voltage is compromised. In the opposite case, where the overpotential is too small, carrier injection is slowed down, resulting in a loss of current.[1] Finding the perfect match is difficult owing to the fact that the selective contact must fulfill other desirable requirements, such as high carrier mobility, transparency, high crystallinity, and material availability, often leaving a limited choice of materials. One possible method of manipulating band alignments is by the introduction of a dipole layer at the contact between the sensitizer and the selective contact. This has been successfully applied in various solar cell realizations via the use of organic dipole layers.[2−4]

It was shown that the energy level of either the photoanode or cathode can be modified by the adsorption of molecular dipoles.[5−7] Moreover, a systematic manipulation of the QDs sensitizer energy levels in QD sensitized solar cells (QDSSCs) was demonstrated using the same principle by adsorbing benzenethiol and acid derivatives molecules with different molecular dipole moments.[8,9] The dipole moments achievable by molecular dipoles are usually relatively small. This led us to explore the applicability of an alternative method for shifting the energy levels of semiconductors by using the photoinduced dipole (PID) phenomenon. We recently showed that by using colloidal ZnSe/CdS type-II core/shell structure QDs deposited on CdS sensitizer layer on a mesoporous TiO_2 photoanode, the accumulated negative charges in the TiO_2 and positive ones in the cores of ZnSe type-II QDs create a relatively strong dipole across the CdS sensitizer layer, inducing a negative shift of the TiO_2 energy bands, which results in higher V_{oc}.[10] The same principle is responsible for the increased photovoltage observed from type-II CdTe/CdSe sensitized solar cells relative to their type-I counterparts, leading to one of the most efficient QD-sensitized cells ever fabricated.[11,12]

Here we provide a detailed study of the PID effect using a planar photovoltaic cell architecture. This allows us to quantitatively characterize the underlying transient dynamics initiated by photoexcitation of the type-II QD layer as well as its global effect on the cell performance. To do this, we needed to design an experimental system that fulfills the following conditions: First, it must have a planar structure to simplify the quantitative analysis. Second, it must be a system where the dipole-induced changes in the photovoltage will be decoupled from the cell photocurrent, the latter being mainly controlled by the optical density of the cell. Third, the system must allow for turning the PID effect on and off in a controlled manner, enabling the separation of the different functions in the cell. For this end, we construct here a system that allows for spectral selection, where the cell can operate with red light, but the PID effect is only activated under green illumination. This design enables us to investigate the PID effect in a more quantitative manner, as described in detail in the following. Furthermore, it provides a deeper understanding of the charge transport and

Received: June 29, 2014
Accepted: July 18, 2014
Published: July 18, 2014

   dx.doi.org/10.1021/jz501336r | J. Phys. Chem. Lett. 2014, 5, 2717−2722

buildup time scales in the cell that will allow for elaborate design of more efficient cells in the future.

Herein we utilize type-II QDs absorbing only a portion of the solar spectrum to manipulate the energy level alignment between the TiO_2 and the electrolyte while optimizing the photovoltage and photocurrent outputs of the solar cell. Thus, in principle, we manage to separate the cell into two different functions. One is the CdSe sensitizing layer generating the photocurrent, while the second is the type-II QDs layer providing additional control of the photovoltage by the PID effect. This is realized by depositing a monolayer of type-II QDs with an engineered energy band alignment on top of the CdSe sensitizer layer using a planar thin film solar cell configuration. Figure 1 shows a schematic illustration of the

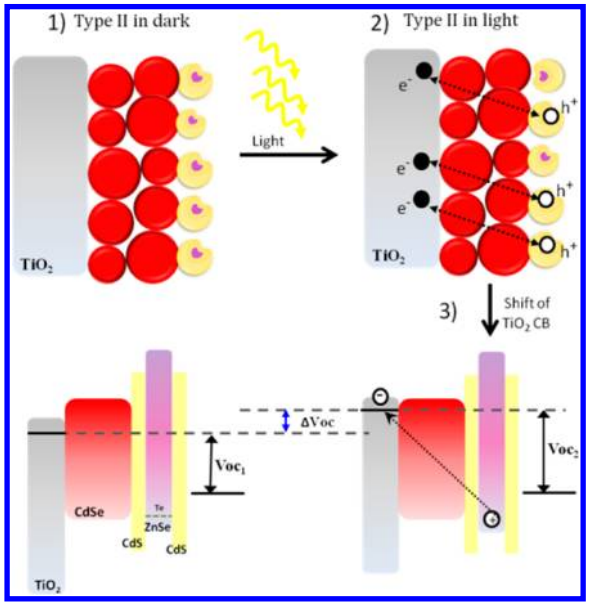

Figure 1. Schematic illustration of the photoinduced-dipole quantum-dot-sensitized solar cells composed of dense TiO_2, CdSe sensitizer layer and a monolayer of ZnSe:Te/CdS type-II QDs. (1) and (2) are cells under dark and under illumination, respectively. (3) Band diagram of the cell. When the type-II QDs undergo photoexcitation, they create a strong dipole that negatively shifts the TiO_2 conduction band energy.

PID system. Steps (1) and (2) of Figure 1 show the PID cell under dark and under illumination, respectively. Figure 1 step (3) demonstrates the energy level diagram of the PID cell showing its working principle. Upon photoexcitation of the ZnSe:Te/CdS core/shell type-II QDs, electrons are injected through the CdS shell to the CdSe sensitizer layer and from there to the dense TiO_2, while the holes are transiently trapped in the QD core before being scavenged by the electrolyte. The deep Te dopant level in the ZnSe core along with the energy barrier provided by the CdS shell enables us to slow down hole scavenging by the electrolyte in a controlled manner.[13,14] In this situation, accumulation of negative charges in the TiO_2 (electron conductor) and a partial population of positive ones in the ZnSe:Te cores negatively shifts the TiO_2 energy bands relatively to the electrolyte, resulting in higher cell photovoltage.

Thin-film electrodes of dense nano crystalline TiO_2 were deposited onto a fluorine-doped tin oxide (FTO) conductive glass by spray pyrolysis. On top, a CdSe layer was grown by chemical bath deposition (CBD), forming a good contact that allows efficient injection of electrons into the TiO_2 conduction band (CB). The electrode was then treated in a solution of 1,4-benzenedithiol to serve as linkers for the ZnSe:Te/CdS type-II QDs deposition. ZnSe:Te/CdS type-II QDs were synthesized according to the protocol of Deutsch et al.[15] Following, all cells were coated with ZnS by the successive ion layer adsorption and reaction (SILAR) method. The cells were measured using an aqueous polysulfide redox electrolyte and a PbS counter electrode to form a sandwich-type cell.[16] A cell consisting of only a dense planar TiO_2 with the common CdSe sensitizer layer was used for reference. The cell that is identical to the reference one but in addition contains a monolayer of colloidal type-II ZnSe:Te/CdS QDs chemically adsorbed on the CdSe sensitizer layer is referred to as the PID cell.

Figure 2 shows the $I-V$ performance, measured under AM 1.5 illumination for the PID (blue) and the reference (red)

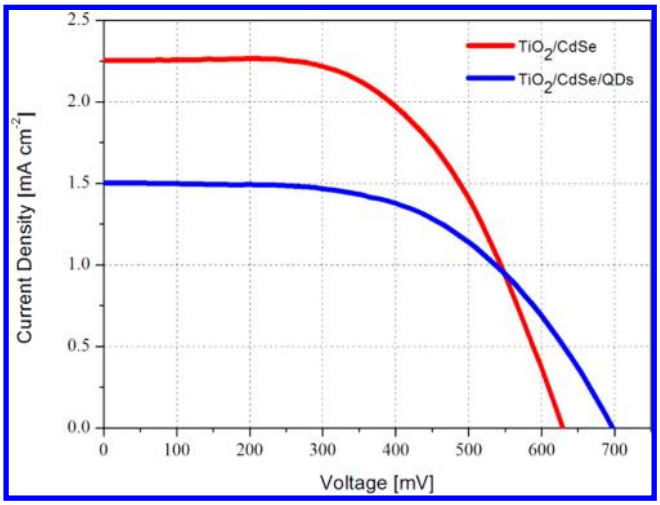

Figure 2. $I-V$ characteristics of the ZnSe:Te/CdS type-II QDs (i.e., the PID cell) in blue clearly showing an increase in the open circuit-voltage compared with the reference cell in red.

cells. The PID cell gives ~75 mV increase in V_{oc} relative to the reference cell. Concomitantly, the photocurrent is lower for the PID cell because of the decrease in driving force for electron injection caused by the initially small overpotential between the TiO_2 CB and CdSe CB, which is estimated to be ~100 mV.[8,17] Notably, a similar increase in photovoltage accompanied by a decrease in photocurrent is obtained for similarly designed mesoporous CdSe-sensitized cells. (For more information, see the Supporting Information.)

To gain better understanding of the physical properties of the PID effect and its limitations, a quantitative study of the QD layer density was performed. Figure 3a shows a high-resolution scanning electron microscope (HR-SEM) micrograph cross-section of the cell. The measured average thickness of the dense TiO_2 was ~170 nm, while the CdSe layer thickness was ~100 nm. The size of the type-II QDs extracted from both their absorption spectrum and TEM images (Figure 3b, green line) is ~5 nm in diameter. Their number density was estimated by measuring the zinc content by inductive coupled plasma atomic emission (ICP-AE) spectroscopy. Overall, we found a very high surface coverage of the ZnSe:Te/CdS type-II QDs, reaching ~90% of the "flat" area of the electrode (neglecting its roughness). In addition, Figure 3b shows the absorbance spectra of the reference cell and the PID cell, indicating that QD adsorption hardly modifies the optical

dx.doi.org/10.1021/jz501336r | J. Phys. Chem. Lett. 2014, 5, 2717−2722

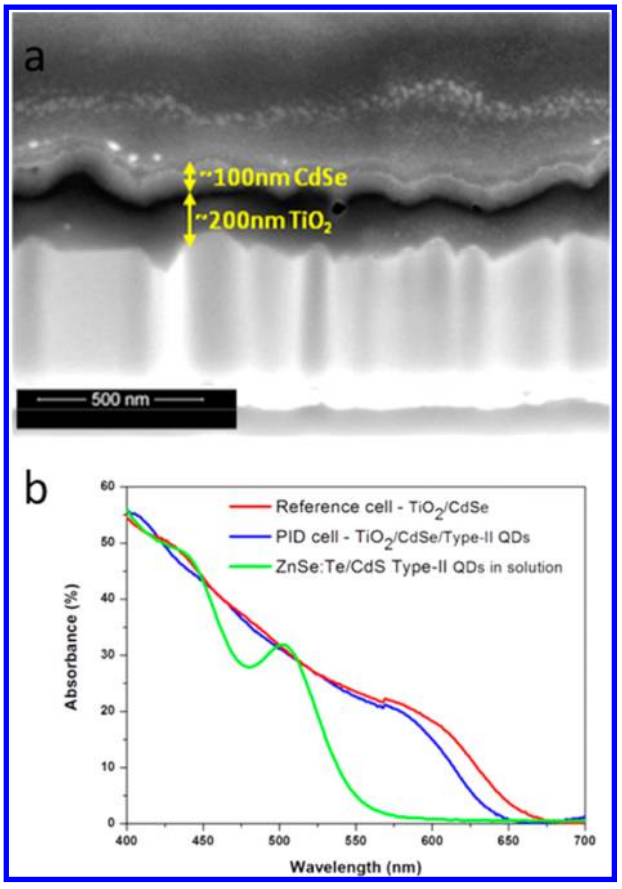

Figure 3. (a) Cross-section image of the dense TiO_2/CdSe layers. The thickness of TiO_2 and CdSe is 140−220 and 100 nm, respectively. (b) Absorption spectra of the reference electrode (red), the PID electrode (blue), and the ZnSe:Te/CdS type-II QDs in solution (green).

density of the cell (and the photogenerated carrier density). The CdSe absorbance onset at ∼650 nm is red-shifted with respect to the QDs (which start absorbing light at ∼570 nm, as can be seen in Figure 3b). This enables the separate excitation of the CdSe sensitizer and the QDs by controlling the excitation wavelength.

A charge-extraction measurement was conducted to verify that the increase in V_{oc} in the PID cell indeed is a result of the TiO_2 CB being pushed up by the PID effect and not due to charge build up in the anode. In this measurement, the cells are subject to a variable light under open circuit conditions. When a steady V_{oc} is reached at specific illumination intensity, the cell is short circuited via a known resistor to collect the accumulated charge within the electrode. Figure 4 shows the accumulated charge density as a function of steady-state V_{oc}. It is clearly seen that the photovoltage in the PID cell (Figure 4, blue circles) is ∼130 mV higher than that for the reference cell (Figure 4, red circles) for the same charge density in the TiO_2 electrode. This also stands in good agreement with the V_{oc} values difference observed in the $I-V$ measurements. Furthermore, when selectively exciting only the CdSe sensitizer by using a 625 nm long-pass filter (Figure 4, green triangles), the V_{oc} is reduced to nearly its value in the reference cell, where no type-II QDs are present. We believe that the shift is not complete because of possible hole transfer from the CdSe layer to the type-II QDs resulting in a small PID effect.

The increase in V_{OC} depends on the areal density of holes in the type-II QDs. Once the holes are scavenged by the

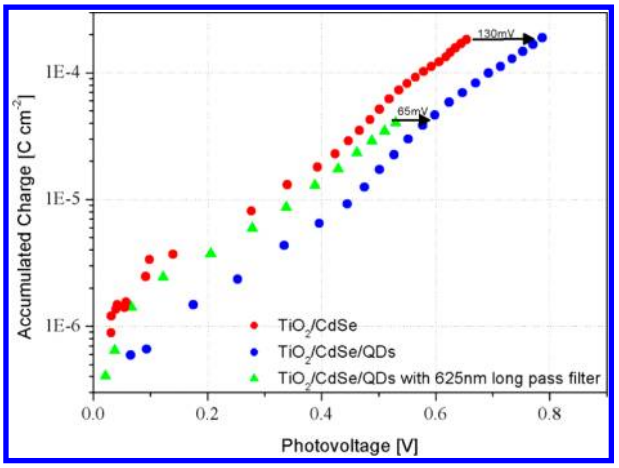

Figure 4. Accumulated charge as a function of the photovoltage for the reference cell containing only dense-TiO_2/CdSe (red) and the PID cell containing dense-TiO_2/CdSe/ZnSe:Te/CdS type-II (blue). In the PID cell, the accumulated charge for the same V_{oc} decreases, indicating that the TiO_2 energy bands were negatively shifted due to the formation of the dipole moment. In green, the PID cell measured with a 625 nm long-pass filter illuminating only the CdSe layer, showing that the TiO_2 is positively shifted, converting back to nearly the reference cell values.

electrolyte, they are screened and no longer contribute to the PID. Under continuous illumination, the areal density is determined by a steady-state condition: the rate of hole harvesting from the type-II QDs by the electrolyte must equal their rate of generation by the illuminating light. The magnitude of the PID is therefore determined by the lifetime of the holes confined in the type-II cores. Transient photovoltage measurements should allow direct experimental access to this important parameter of the PID cell. The schematic of the experiment is shown in Figure 5. The PID cell was illuminated with a 636 nm red CW laser, exciting only the CdSe layer with power density sufficiently high to nearly reach the maximal achievable V_{oc} of the cell. Under these conditions, the cell is illuminated by an additional intense short pulse at 532 nm. Following this, there is an increase in V_{oc} due to two mechanisms. The first is the increased carrier generation in the sensitizer layer, which is expected to be small as the V_{oc} is close to its saturation value. The second is due to activation of the PID where electrons from the QDs shell are injected into the TiO_2 photoanode across the CdSe layer serving here in effect also as a dielectric layer while the holes are trapped in the ZnSe:Te cores.

Figure 6 shows transient photovolatge for the PID cell in blue and the reference cell in red relative to the reference V_{oc} under red excitation only. Clearly, the PID cell shows a dramatic increase in V_{oc} of ∼100 mV, which decays on a submillisecond time scale. The PID cell data were fitted with a three-exponent decay with excellent fitting quality, as shown in the inset of Figure 6. The decay transient of the reference cell where the initial fast process does not exist is easily fitted by a biexponential function. The extracted fitting parameters that are presented in Table 1 show a complete separation of time scales between the carrier recombination processes. The two fast components in the PID cell, totaling ∼100 mV voltage increase, decay on an average time scale of ∼270 μs (summing up the two fast components; see Table 1). This fast initial component is completely absent in the reference cell and thus can be attributed solely to the PID decay due to the hole-electrolyte

dx.doi.org/10.1021/jz501336r | J. Phys. Chem. Lett. 2014, 5, 2717−2722

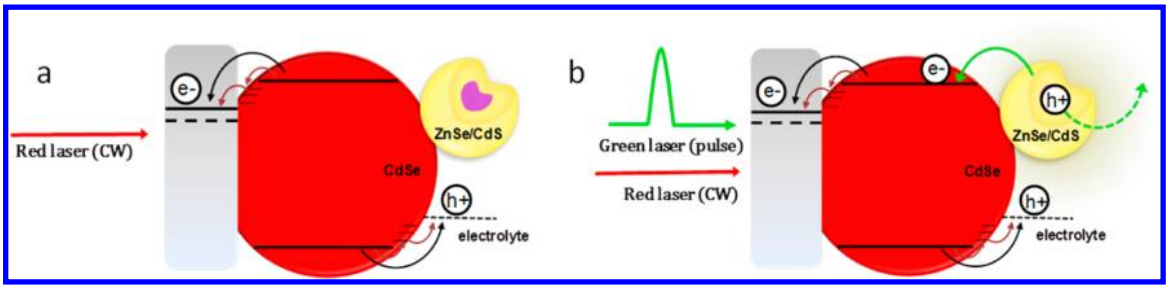

Figure 5. Illustration of the transient photovoltage measurement scheme and energy band diagrams showing the charge-transfer processes in the PID cell. (a) PID cell is illuminated by a 636 nm CW laser, exciting only the CdSe, resulting in electron injection from the CdSe CB directly to the TiO_2 CB, while holes are removed by the electrolyte. (b) Addition of a 532 nm pulsed laser illuminates both CdSe QDs and the type-II QDs. The electrons in the CdS shell of the type-II QDs are injected into the CdSe and the TiO_2, while the holes stay trapped inside the Te-doped ZnSe cores. As a result, a capacitor-like device is created across the CdSe layer, which generates a large photoinduced dipole (PID).

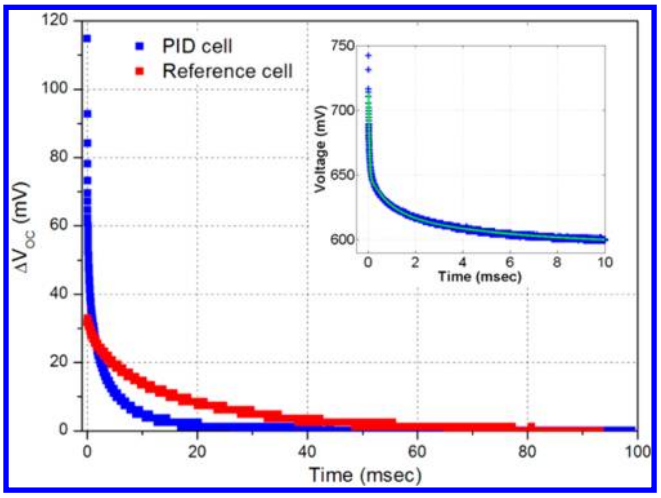

Figure 6. Transient photovoltage measurements showing a large rise in photovoltage that is observed only for the PID cell (blue) compared with the reference cell (red). Moreover, it is clearly seen that an initial rapid transient component appears (~100 meV extra), indicating that hole regeneration in the type-II QDs occurs within tens of microseconds. Inset: Transient photovoltage measurement for the PID cell in blue and the fitting of the data with a three exponent decay equation in green.

Table 1. Transient Photovoltage Measurements Fitting Parameters for the Reference and the PID Cells

	PID cell		reference cell	
decay process	ΔV_{oc} (mV)	t (ms)	ΔV_{oc} (mV)	t (ms)
holes−electrolyte regeneration	68	0.04	0	0
	28	0.82	11	3.9
direct (e-h) recombination across the cell	26	5.27	21	22.46

regeneration dynamics of holes confined in the type-II QDs. The distribution of time scales leading to a second fast component may be due to inhomogeneous effects among the type-II QDs or due to hole transfer from the CdSe layer to the QD cores. The third, slow, few-millisecond component arises from electron−hole direct recombination of electrons either in the TiO_2 CB or in the CdSe-sensitizer layer with residual holes in the polysulfide electrolyte.[8,18] The shorter lifetime of this process in comparison with the reference can be related to the electron−hole recombination between electrons in the TiO_2 and residual long-lived holes in the type-II QDs cores. Similar dynamics demonstrating those two recombination processes were recorded before for CdSe QDSSC and DSSC.[19] Note that for the slow recombination process, the V_{oc} increase is very small relative to the faster components. This proves that the main contribution to photovoltage increase indeed comes from the PID effect and is governed by the dynamics of hole transfer from the type-II QDs to the electrolyte.

The hole lifetime extracted from the charge-extraction measurement allows us to provide an independent prediction of the expected increase in V_{oc} based on the assumption that the PID effect is analogous to a plate capacitor. The expected average number of charges per type-II QD is estimated using the simple parallel plate capacitor equation

$$Q = \frac{\varepsilon \cdot \varepsilon_0 \cdot A}{d} \cdot V$$

where ε is the dielectric constant of bulk CdSe, ε_0 is the vacuum permittivity, A is the area of the electrode, and d is the thickness of the CdSe dielectric layer. V is taken as 100 mV, the extra photovoltage measured in the charge extraction measurement for the PID cell. Dividing the total additional PID charge by the number of type-II QDs gives a charge density of 0.02 holes per QD. This means that on average only 1 of 50 QDs holds a dipole contributing to the PID effect.

As a consistency check, the photon absorption rate at a photon flux of 1.5AM was calculated for the PID cell by measuring the absorption cross section of the type-II QDs, giving ~100 absorbed photons per second per single dot.[11] This translates to a 10 ms time separation between consecutive photocharging events. This time scale is a factor of ~40 longer than the 270 μs lifetime of the photogenerated hole extracted from the transient photovoltage measurement, corresponding to an excitation level of one photogenerated dipole for every 40 QDs on average. Thus, these two independent measurements, transient photovoltage and the extracted charge density from the open-circuit voltage increase, yield consistent estimates to the average charge of the type-II QDs.

To conclude, we showed that the photovoltage can be increased significantly by the addition of a PID layer. We revealed the underlying dynamics and magnitude of the different mechanisms contributing to the photovoltage increase. We showed that this increase is governed by the PID effect and the dynamics of the hole−electrolyte regeneration rate. This was achieved by spectrally separating the cell excitation with that inducing the PID effect. The PID effect provides a new knob for in situ, illumination-dependent control of the open circuit voltage of the cell. Moreover, there are multiple ways that allow for control of its magnitude, such as the QD

dx.doi.org/10.1021/jz501336r | J. Phys. Chem. Lett. 2014, 5, 2717−2722

concentration and hole lifetime (determined, in turn, by QD properties such as the shell thickness and doping level). Consequently, there is significantly more freedom for optimization of the band alignment, and consequently the photovoltage and the photocurrent in the cell, under working conditions. This concept has a potential to be implemented in other PV technologies such as solid-state QDSSCs and perovskite solar cells to better tune the cell performance.[20−26]

EXPERIMENTAL METHODS

Type-II QDs Synthesis. ZnSe:Te/CdS cores synthesis: The synthesis is done in a noncoordinating solvent, in a one-pot approach. Typically, a mixture of 3 mL of octadecene (ODE) and 4 mL of hexadecylamine (HDA) are put in a flask and put under vacuum at 120 °C for 1 h. 0.2 mmol of selenium and 0.01 mmol of tellurium are dissolved in 2 mL of trioctylphosphine (TOP) and are injected at 120 °C to the flask. The temperature is then raised to 270 °C, and 0.2 mmol of diethylzinc (DEZ) in ODE is injected. The synthesis is monitored by an absorption measurement. After ∼10 min, the reaction reaches completion, as observed from the shift of the exciton peak in the absorbance. The temperature is then lowered to 180 °C, and the sulfur and cadmium precursors are added dropwise until the desired particle size is reached. The sulfur precursor is prepared from elemental sulfur in ODE at a concentration of 0.1M, and for cadmium we used a solution of 0.1 M cadmium oleate in ODE. The dots were then precipitated with toluene and methanol and redissolved in toluene. All chemicals were purchased from Sigma-Aldrich.

TiO_2/CdSe Electrodes Preparation. Dense compact TiO_2 layer was prepared by spray pyrolysis on FTO-covered glass substrate at 450 °C using compressed air as a carrier gas. For the CdSe deposition, a seeding layer of CdS was deposited by the SILAR method prior to the CdSe sensitization. Therefore, the TiO_2 electrode was dipped into 0.1 M $Cd(NO_3)_2$ for 1 min, washed with deionized water, immersed into 0.1 M Na_2S aqueous solution, and washed again. After seeding, CBD was used to sensitize the electrode with CdSe QDs. Sodium selenosulfate (Na_2SeSO_3) solution (80 mM) was prepared by dissolving Se powder in a 200 mM Na_2SO_3 solution (solution A). $CdSO_4$ (80 mM) and tri sodium salt of nitrilotriacetic acid ($N(CH_2COONa)_3$) (120 mM) were mixed in a volume ratio 1:1 (solution B) before solutions A and B were mixed in a volume ratio 1:2. The TiO_2 electrode were immersed into the final solution for 24 h at 10 °C and kept in the dark.

Type-II QDs Deposition. The TiO_2/CdSe electrodes were immersed in a solution of 1,4-benzenedithiol in methanol overnight, washed with methanol and toluene, and then immersed in a solution of ZnSe:Te/CdS type-II QDs in toluene over several days. Lastly, the electrodes were washed with toluene dried under N_2 and kept under an inert atmosphere until measured.

ZnS Coating. A ZnS coating was applied both to the PID and reference cells. Typically, the electrodes were immersed sequentially in a 0.6 g of zinc acetate hydrate dissolved in 25 mL of deionized water and then in 0.2 g sodium sulfide hydrate in 25 mL of deionized water, 1 min each with washing in deionized water in between. Two cycles were performed.

I−V Measurement. Photocurrent voltage characteristics were performed with an Eco-Chemie potentiostat. A solar simulator class A (Newport) calibrated to 100 mW/cm^2 (AM 1.5 spectrum) served as a light source. The illuminated area of the cell was set to 1.03 cm^2 using an aperture. Na_2S (1 M), 0.1 M sulfur, and 0.1 M KOH solution served as the electrolyte. A PbS foil was used as a counter-electrode.

Absorption Measurement. The absorption spectra of the electrode were measured using a Varian spectrophotometer equipped with an integrating sphere.

Focused Ion Beam Cross Section. A cross section of the electrodes was performed using a Helios 600, dual beam scanning electron microscopy (SEM), and focused ion beam (FIB) instrument.

Charge-Extraction Measurement. For charge-extraction measurements, the solar cell was connected to a data acquisition under open-circuit conditions. Then, the device was illuminated with white light to a desired V_{oc}, at this point, equilibrium between charge formation, due to the illumination with light, and charge recombination was reached. Then, the light was turned off simultaneously to short-circuiting the cell through a 10Ω resistor so that the total charge flow can be derived from integration of the current measurement through the cell.

Transient Photovoltage Measurement. A red CW 636 nm diode laser (Coherent Cube) illuminated the complete solar cell. The excitation power was set so as to reach the maximum V_{oc}. Following, the cell was illuminated with an additional green 532 nm Q-switched laser emitting 5 ns pulses at a repetition rate of 10 Hz. The transient photovolatge was measured with an Autolab potentiostat (PGSTAT302N) equipped with a fast module (ADC10M).

ASSOCIATED CONTENT

Supporting Information

Mesoporous PID cells and their photovoltaic properties. This material is available free of charge via the Internet at http://pubs.acs.org.

AUTHOR INFORMATION

Corresponding Author

*E-mail: dan.oron@weizmann.ac.il.

Author Contributions

§M.K. and S.B. contributed equally

Notes

The authors declare no competing financial interest.

ACKNOWLEDGMENTS

A.Z. thanks the Israel Strategic Alternative Energy Foundation (I-SAEF) for the financial support. S.B. is grateful for the support of the Adams Fellowship Program of the Israel Academy of Sciences and Humanities. D.O. acknowledges financial support from the Leona M. and Harry B. charitable trust, the Weizmann institute Alternative Energy Research Initiative. and the Crown center of Photonics.

REFERENCES

(1) Robel, I.; Kuno, M.; Kamat, P. V. Size-Dependent Electron Injection from Excited CdSe Quantum Dots into TiO_2 Nanoparticles. *J. Am. Chem. Soc.* **2007**, *129*, 4136−4137.

(2) Visoly-Fisher, I.; Sitt, A.; Wahab, M.; Cahen, D. Molecular Adsorption-Mediated Control over the Electrical Characteristics of Polycrystalline CdTe/CdS Solar Cells. *ChemPhysChem* **2005**, *6*, 277−285.

(3) Goh, C.; Scully, S. R.; McGehee, M. D. Effects of Molecular Interface Modification in Hybrid Organic-Inorganic Photovoltaic Cells. *J. Appl. Phys.* **2007**, *101*, 114503.

(4) Barea, E. M.; Shalom, M.; Giménez, S.; Hod, I.; Mora-Seró, I.; Zaban, A.; Bisquert, J. Design of Injection and Recombination in

Quantum Dot Sensitized Solar Cells. *J. Am. Chem. Soc.* **2010**, *132*, 6834−6839.
(5) Hod, I.; Tachan, Z.; Shalom, M.; Zaban, A. Characterization and Control of the Electronic Properties of a NiO Based Dye Sensitized Photocathode. *Phys. Chem. Chem. Phys.* **2013**, *15*, 6339−6343.
(6) Lee, Y.-L.; Chi, C.-F.; Liau, S.-Y. CdS/CdSe Co-Sensitized TiO_2 Photoelectrode for Efficient Hydrogen Generation in a Photoelectrochemical Cell. *Chem. Mater.* **2010**, *22*, 922−927.
(7) Chi, C.-F.; Cho, H.-W.; Teng, H.; Chuang, C.-Y.; Chang, Y.-M.; Hsu, Y.-J.; Lee, Y.-L. Energy Level Alignment, Electron Injection, and Charge Recombination Characteristics in CdS/CdSe Cosensitized TiO_2 Photoelectrode. *Appl. Phys. Lett.* **2011**, *98*, 012101.
(8) Rühle, S.; Greenshtein, M.; Chen, S.-G.; Merson, A.; Pizem, H.; Sukenik, C. S.; Cahen, D.; Zaban, A. Molecular Adjustment of the Electronic Properties of Nanoporous Electrodes in Dye-Sensitized Solar Cells. *J. Phys. Chem. B* **2005**, *109*, 18907−18913.
(9) Shalom, M.; Rühle, S.; Hod, I.; Yahav, S.; Zaban, A. Energy Level Alignment in CdS Quantum Dot Sensitized Solar Cells Using Molecular Dipoles. *J. Am. Chem. Soc.* **2009**, *131*, 9876−9877.
(10) Buhbut, S.; Itzhakov, S.; Hod, I.; Oron, D.; Zaban, A. Photo-Induced Dipoles: A New Method to Convert Photons into Photovoltage in Quantum Dot Sensitized Solar Cells. *Nano Lett.* **2013**, *13*, 4456−4461.
(11) Itzhakov, S.; Shen, H.; Buhbut, S.; Lin, H.; Oron, D. Type-II Quantum-Dot-Sensitized Solar Cell Spanning the Visible and Near-Infrared Spectrum. *J. Phys. Chem. C* **2013**, *117*, 22203−22210.
(12) Wang, J.; Mora-Seró, I.; Pan, Z.; Zhao, K.; Zhang, H.; Feng, Y.; Yang, G.; Zhong, X.; Bisquert, J. Core/shell Colloidal Quantum Dot Exciplex States for the Development of Highly Efficient Quantum-Dot-Sensitized Solar Cells. *J. Am. Chem. Soc.* **2013**, *135*, 15913−15922.
(13) Zhang, L.; Lin, Z.; Luo, J.-W.; Franceschetti, A. The Birth of a Type-II Nanostructure: Carrier Localization and Optical Properties of Isoelectronically Doped CdSe:Te Nanocrystals. *ACS Nano* **2012**, *6*, 8325−8334.
(14) Sonawane, K. G.; Rajesh, C.; Temgire, M.; Mahamuni, S. A Case Study: Te in ZnSe and Mn-Doped ZnSe Quantum Dots. *Nanotechnology* **2011**, *22*, 305702.
(15) Avidan, A.; Deutsch, Z.; Oron, D. Interactions of Bound Excitons in Doped Core/shell Quantum Dot Heterostructures. *Phys. Rev. B* **2010**, *82*, 165332.
(16) Tachan, Z.; Shalom, M.; Hod, I.; Rühle, S.; Tirosh, S.; Zaban, A. PbS as a Highly Catalytic Counter Electrode for Polysulfide-Based Quantum Dot Solar Cells. *J. Phys. Chem. C* **2011**, *115*, 6162−6166.
(17) Markus, T. Z.; Itzhakov, S.; Cahen, D.; Hodes, G.; Oron, D.; Naaman, R. Energetics of CdSe Quantum Dots Adsorbed on TiO_2. *J. Phys. Chem. C* **2011**, 13236−13241.
(18) Zewdu, T.; Clifford, J. N.; Hernández, J. P.; Palomares, E. Photo-Induced Charge Transfer Dynamics in Efficient TiO_2/CdS/CdSe Sensitized Solar Cells. *Energy Environ. Sci.* **2011**, *4*, 4633−4638.
(19) Montanari, I.; Nelson, J.; Durrant, J. R. Iodide Electron Transfer Kinetics in Dye-Sensitized Nanocrystalline TiO_2 Films. *J. Phys. Chem. B* **2002**, *106*, 12203−12210.
(20) McDonald, S. a; Konstantatos, G.; Zhang, S.; Cyr, P. W.; Klem, E. J. D.; Levina, L.; Sargent, E. H. Solution-Processed PbS Quantum Dot Infrared Photodetectors and Photovoltaics. *Nat. Mater.* **2005**, *4*, 138−142.
(21) Pattantyus-abraham, A. G.; Kramer, Ḱ. I. J.; Barkhouse, Ḱ. A. R.; Wang, X.; Konstantatos, G.; Debnath, R.; Levina, L.; Raabe, I.; Nazeeruddin, M. K.; Sargent, E. H. Depleted-Hetrojunction Colloidal Quantum Dot Solar Cells. *ACS Nano* **2010**, *4*, 3374−3380.
(22) Yu, P.; Zhu, K.; Norman, A. G.; Ferrere, S.; Frank, A. J.; Nozik, A. J. Nanocrystalline TiO_2 Solar Cells Sensitized with InAs Quantum Dots. *J. Phys. Chem. B* **2006**, *110*, 25451−25454.
(23) Kim, H. S.; Lee, C. R.; Im, J. H.; Lee, K. B.; Moehl, T.; Marchioro, A.; Moon, S. J.; Humphry-Baker, R.; Yum, J. H.; Moser, J. E.; et al. Lead Iodide Perovskite Sensitized All-Solid-State Submicron Thin Film Mesoscopic Solar Cell with Efficiency Exceeding 9%. *Sci. Rep.* **2012**, *2* (591), 1−7.
(24) Burschka, J.; Pellet, N.; Moon, S. J.; Humphry-Baker, R.; Gao, P.; Nazeeruddin, M. K.; Grätzel, M. Sequential Deposition as a Route to High-Performance Perovskite-Sensitized Solar Cells. *Nature* **2013**, *499*, 316−319.
(25) Liu, M.; Johnston, M. B.; Snaith, H. J. Efficient Planar Hetrojunction Perovskite Solar Cells by Vapor Deposition. *Nature* **2013**, *501*, 395−398.
(26) Edri, E.; Kirmayer, S.; Kulbak, M.; Hodes, G.; Cahen, D. Chloride Inclusion and Hole Transport Material Doping to Improve Methyl Ammonium Lead Bromide Perovskite-Based High Open-Circuit Voltage Solar Cells. *J. Phys. Chem. Lett.* **2014**, *5*, 429−433.